2013

Analysis of Polyethylene Glycol in the α-Hemolysin Nanopore

David M. Dancho
Virginia Commonwealth University

Analysis of Polyethylene Glycol in the α-Hemolysin Nanopore

A thesis submitted in partial fulfillment of the requirements for the degree of Masters of Science in Physics / Applied Physics at Virginia Commonwealth University

By: David Dancho

B.S. in Physics

Bloomsburg University, 2011

Major Director:

Joseph E. Reiner, Ph.D., Assistant Professor, Department of Physics

Virginia Commonwealth University

Richmond, Virginia, 23284

Abstract:

Nanopores have been shown to be a useful analytical tool for single molecule detection. They have been used to study the composition of DNA and other molecules of interest. These pores are usually α-hemolysin which is a toxin from *Staphylococcus aureus* or more recently nanoscale synthetic solid state pores. Now we are beginning to look at other molecules or proteins by sending them into the nanopores and measuring a characteristic partial current blockade. In this thesis we look at polyethylene glycol (PEG) as it enters and blocks current through a single alpha hemolysin pore. We report the effects of ionic strength, PEG size, and applied voltage on the depth and duration of the current blockades. We also apply autocorrelation analysis on the arrival times of PEG molecules to the pore see if we can identify if the PEG is translocating through the pore or escaping from the same side it enters. This suggests a new approach to current blockade analysis.

Acknowledgments:

I would like to thank everyone who has helped me with this thesis.

Table of Contents:

Table of Figures:

Chapter 1: Background Information

Single molecule measurements are important because they can tell you information about the distribution of parameters of a molecule and not just the average values that you would obtain from measurements upon an ensemble of molecules. This is useful because now we can see variation between individual molecules under identical conditions. This heterogeneity can be used to better understand the internal properties of a molecule. {1}

A nanopore detector is a nanometer-sized hole in a membrane surrounded by salt water with an applied voltage that will give rise to a current across the hole. As the molecules block the hole they also block the current by adding resistance which will give blockades in the current. In order for these blockades to be measurable we require a few conditions be met. First the hole must remain open and be stable in order for the molecules to freely flow through the hole and so that the current blockades can be associated with molecules entering the hole and not from gating artifacts of the hole itself. Next the volume of the pore sensing region must be small in order to see small molecules if the hole is too large then the small molecules will not have much effect on the current. Finally the molecule must remain in the hole for a couple of 100's of microseconds due to the bandwidth of the detection system which is on the order of 10-100 kHz otherwise the molecule might be missed as it travels through the pore.

Historically DNA has been the main analyte of interest for nanopore sensing applications {2}. This is because almost 20 years ago, researchers discovered that single-stranded DNA could thread through an alpha hemolysin (αHL) nanopore and give rise to detectable current blockades {3}. This created great interest in the field of nanopore sensing because of the implications for low-cost DNA sequencing. Because of this, the alpha hemolysin nanopore has

been used as the workhorse for single molecule nanopore sensing. In addition to DNA sequencing applications, alpha hemolysin has also shown promise in the area of single molecule "mass spectrometry" {4}. Polyethylene glycol (PEG) molecules have been shown to enter the pore and give rise to blockades that can be used to resolve PEG that differs in size by one monomer subunit. This level of sensitivity has sparked interest in using PEG for DNA sequencing applications. {5}

Understanding the mechanism of PEG interactions with the alpha hemolysin nanopore is important because the potential resolving power of the alpha hemolysin/PEG interaction suggests numerous applications in genomics, proteomics and metabolomics. This thesis explores the dependence of the PEG interaction with the alpha hemolysin nanopore under different conditions including, voltage, salt concentration, and PEG concentration.

Alpha Hemolysin (αHL):

The main biological nanopore in use today for nanopore sensing is α-hemolysin, which is a heptameric trans membrane protein of the pathogen *Staphylococcus aureus*. The pore is composed of a cap domain, a stem domain, and seven rim domains. The cap domain is made up of seven β sheets and the amino acids of each of the protomers. The rim domains protrude from the undersides of the heptamer and are in close proximity or in direct contact with the membrane bilayer. Finally the stem domain forms the trans membrane channel that the molecules flow through. The stem is formed of 14 antiparallel β strands, where each protomer contributes two of the strands, and they form a right hand barrel known as a β barrel. The pore itself is roughly 100 Å tall and 100 Å wide with a pore opening of roughly 26 Å. The conductance of the pore displays a linear dependence upon the conductivity of the solution which means that the channel

is water filled. Due to its stable open configuration under trans membrane voltages of up to ~ 150mV alpha hemolysin makes a useful nanopore sensing channel. It also remains stable under high ionic strength solutions like 4M KCL for example. These two facts allow us to clearly separate the molecular blockades from the open channel current. The channel of the pore reversibly closes under conditions of low pH as well as in the presence of divalent and trivalent cations so nanopore sensing is usually done using monovalent cations and neutral pH values. {6}

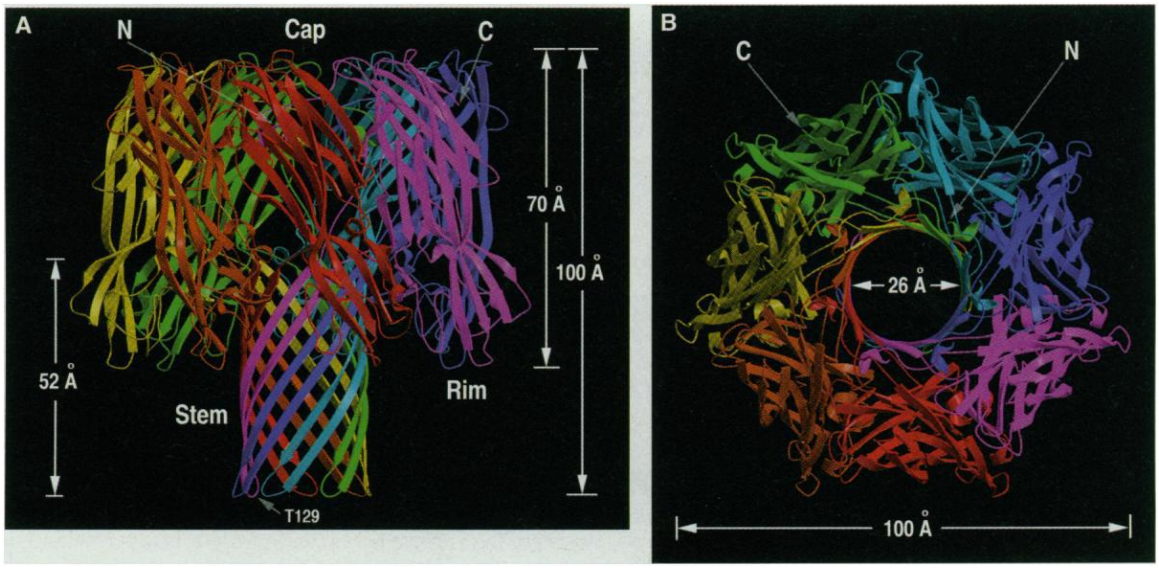

Fig 1: Ribbon representation of α-hemolysin with each protomer in a different color. a) View of pore parallel to the membrane. b) Top view of the pore. Reproduced with permission from {6}.

Another type of nanopore, which we won't discuss in this thesis, is nanoholes which are formed within semiconductor supports. Many groups have developed techniques such as ion beam sculpting, which uses a focused ion beam to form a nanometer sized hole in a silicon nitride support {7}. These pores can work in a large range of electrolytes; they also remain open over a larger range of applied voltages. They can also function under different extremes of pH, temperature, ionic concentration and mechanical stress. In addition, solid state nanopores are manmade so the diameter of the pore can be specifically adjusted when the pores are formed.

Solid state pores do have some downsides such as increased measurement noise and the difficulty of designing the appropriate surface chemistries to bind a particular analyte in solution {7}. The protein sequence of alpha hemolysin nanopores has been identified {6} so that single point mutations can be inserted to allow for precisely engineered sensing characteristics at the single amino acid limit. In summary, alpha hemolysin nanopores provide a number of advantages over solid state pores and so we will choose to focus on the αHL system for the duration of this thesis.

Polyethylene Glycol (PEG)

The analyte molecule we have been working with is polyethylene glycol (PEG) which is a polyether compound with the following chemical formula $H\text{-}(O\text{-}CH_2\text{-}CH_2)_n\text{-}OH$. The formula for the molecular weight of a PEG molecule with *n* repeat units is (44*n*+12) Da which shows that the size and weight of the molecule is parameterized by the repeat unit *n*. Ethylene glycol is a colorless and odorless dihydroxy alcohol that is used as an antifreeze and coolant hydraulic fluid. It is soluble in water and mostly soluble in alcohol and other organic solvents {8}. Most PEG mixtures are parameterized by a mean molecular weight, which in reality corresponds to a distribution of different *n*-sized molecules.

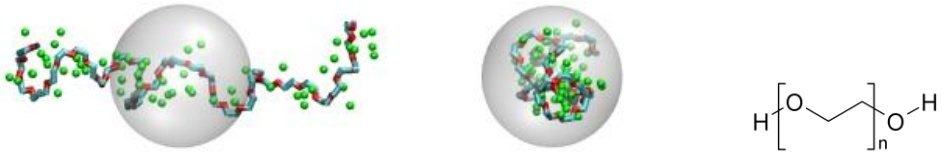

Fig 2: Structure of Polyethylene Glycol {9}. Left and middle head on and cross section view of a PEG 36 molecule where the clear spheres represent the hydrodynamic radius centered at the center of mass. The chemical formula is shown to the right {10}. The bead is a hydrodynamic sphere meant to represent the diffusion of the PEG model which in this case has a diameter of ~ 0.23 nm. Figure reproduced with permission from ref {9}

The importance of the PEG molecule in the field of nanopore sensing results from the strong interactions it has with the interior of the alpha hemolysin nanopore. This interaction gives rise to long-lived current blockades which can be used to extract information about the nanopore or even the PEG molecules themselves {11}. In pure water, PEG molecules are uncharged polymers that, unlike DNA, can be thought of as sequence-less polymers that may inform us about the polymer chain kinetics involved in nanopore sensing. This motivates the study of PEG/αHL interactions in order to better understand these interactions.

Chapter 2: Nanopore sensing

Principle of operation

Nanopore sensing requires the isolation of a single nanopore in a membrane that partions an electrolyte solution. A voltage is applied across the membrane which leads to a detectable open state current, i_{open} or i_o. When a molecule enters the nanopore it leads to a reduction in the current which we refer to as a current blockade. The figure below shows a schematic drawing of the principle of operation. The molecules diffuse in solution outside the nanopore region and enter the pore at random times at a rate that is linearly dependent on the molecule's concentration, diffusion coefficient, and the pore diameter.

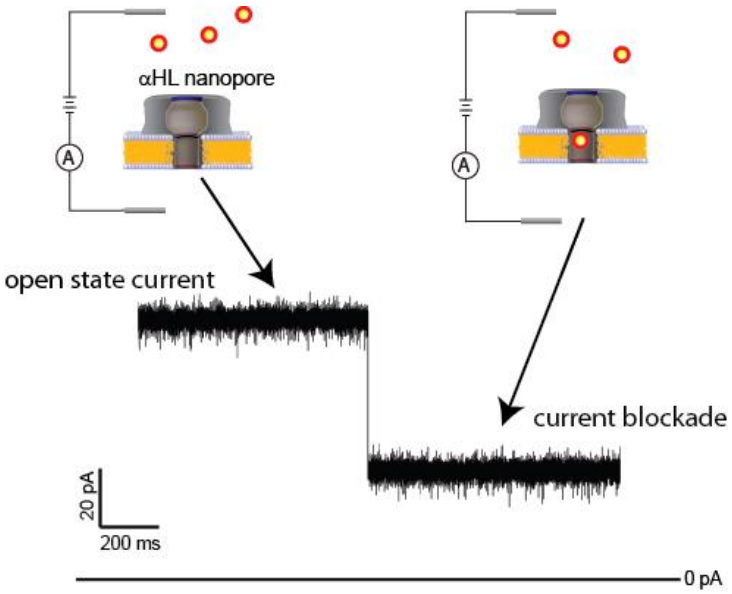

Fig 3: (Left) Current is driven through an alpha hemolysin nanopore and upon the entry of a single molecule (Right) leads to measurable current blockades. Image reproduced from {12}

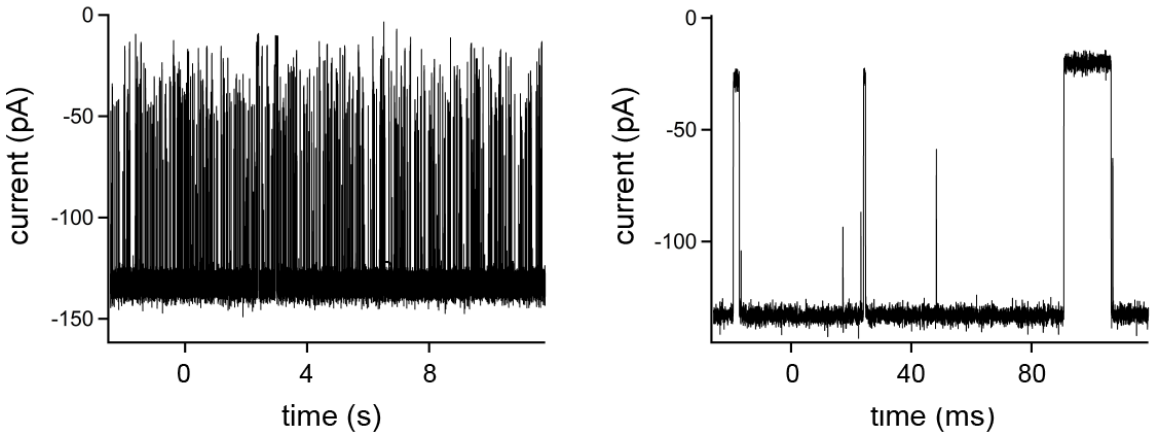

Fig 4: (Left) An approximately 10 second time trace that shows a polydisperse mixture of PEG molecules interacting with a single alpha hemolysin nanopore (PEG 1000, 1500 are at 10 µM and PEG 29 is at 2µM). (Right) Shows a zoomed in view of the individual blockades. We can see that the applied voltage is negative which gives rise to a negative open state current. This is a polarity configuration and for the data the blockades are positive going. The KCL concentration is 3.5M and applied voltage is 40 mV.

Figure 4 shows current time traces over an extended and a short period of time. We measure the current blockade depth blockade duration or residence time, and the arrival time of each PEG molecule. Figure 5 shows the analysis of a single blockade.

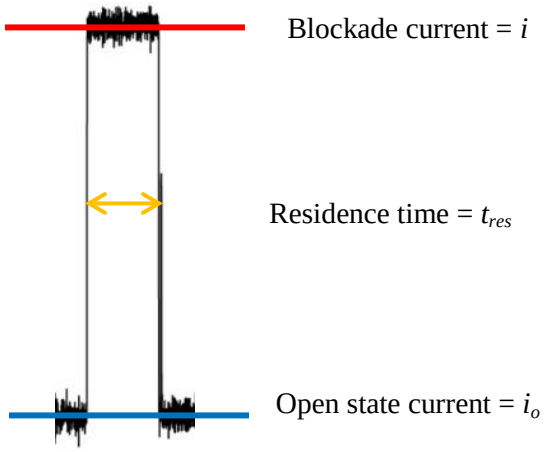

Fig 5: A single blockade event with the blockade depth and duration are shown. Here the applied voltage is negative so the blockades are positive. The analysis is performed by creating histograms of the ratio $\langle i \rangle / \langle i_o \rangle$ for each event where the brackets imply a time average. In addition we record the duration or residence time, t_{res}, of each event.

The blockades are caused by PEG molecules entering and blocking the flow of ions through the nanopore. It appears that the residence times of the blockades are proportional to the length of the molecule, which makes sense since longer molecules should take longer to pass through the pore. The lifetimes of the blockades should be inversely proportional to the applied voltage since the higher voltage will push the molecules faster. The length of the events have also been found to correlate to the molecular weight of the molecule since a molecule with higher molecular weight will most likely be longer then a molecule with lower molecular weight. The frequency of the blockades of these molecules are linked to the concentration since at lower concentrations on average it takes longer for the molecules to make their way to the pore since they are more spread out in the volume. On the other hand higher concentrations will give rise to a higher local concentration close to the pore. {3}

Chapter 3: Experimental Setup Analysis

Experimental Setup

The experiments were performed on an air floated 3x4 ft^2 optical table that was enclosed within a Faraday cage to reduce low frequency electronic ambient noise. The apparatus containing the membrane and reservoirs of salt concentration and PEG concentration was placed on top of an inverted, bright-field microscope. The electrode and protein pipette were positioned into place using manipulators.

The membrane is an approximately 1 cm diameter Teflon sheet that is 25 microns thick. The sheet has a single 100 micron hole over which lipid bilayer membranes are formed. This Teflon sheet was cleaned using foamed tips soaked in pentane inside a chemical hood until there was no remnants of epoxy from the previous run left. The Teflon was then attached to a separately machined Teflon holder using PDMS making sure to center the hole in the Teflon sheet over the hole in the Teflon holder. The Teflon sheet was treated with a pre paint mixture of 1 mg/ml of 1, 2-diphytanoyl-sn-glycero-3-phosphocholine (DPHyPC) in pentane on both sides of the Teflon to facilitate the formation of a stable bilayer membrane across the 100 micron hole. The Teflon holder with the Teflon attached was then mounted on a glass slide holder and positioned onto a manual microscope stage manipulator. Solutions of KCL premixed with PEG of various molecular weights and concentrations were injected above and below the Teflon holder with 2500 µL in the bottom chamber and 700 µL in the top chamber. A quartz glass tube with a filament that had a 1.0 mm outer diameter and a 0.7mm inner diameter was pulled into a patch pipette electrode with a tip diameter of ca. 1µm using a laser pipette puller (P-2000 Sutter Instruments). The electrode tip was then filled with matching KCL concentration that was used

over and under the Teflon, but no PEG was added to the electrode tip. This guarantees that PEG molecules only enter the nanopore from one side (namely the stem side of alpha hemolysin). An Ag/AgCl electrode wire was placed into the back of the glass pipette electrode and this patch electrode was placed in solution and positioned near the 100 micron hole with motorized manipulators. Next using another pipette filled with our lipid mixture, which was 10 mg/ml of DPhyPC in hexadecane was positioned near the hole. The lipid was then blown out of the pipette into an approximately 50 – 100 micron diameter bubble on the end of the tip and the bubble was brought down onto the Teflon near the hole. Using a glass rod with a ball preformed on the end, the lipid was spread over the hole to create a membrane that was allowed to thin to create a lipid bilayer. The pipette containing the lipid was replaced with one containing a 5 to 1 by volume mixture of BSA to alpha hemolysin wild type. The BSA was added to prevent adhesion of the αHL to the inner walls of the glass micropipette tip. This was positioned near the bilayer membrane and a backing pressure of 20-50 hPA was applied to eject the protein into the bilayer membrane. By applying a voltage across the membrane we were able to see the amount off channels embedding into the bilayer by the amount of current we were receiving through the electrode. After a few hundred αHL nanopores inserted into the bilayer membrane, the electrode patch pipette was positioned on top of the lipid bilayer to find a single protein channel. This was verified by checking the value of the current depending upon the voltage applied. If a single channel was not found the patch pipette was removed from the bilayer and cleaned using pressure and placed back onto the lipid bilayer. This was repeated until a single channel was found with which we could take data using that channel. The data was typically taken with a four-pole Bessel low pass filter at 10 kHz with 50 kHz sampling using proprietary Clampex

software (Molecular Devices) and the data was analyzed using in-house software developed in Labview.

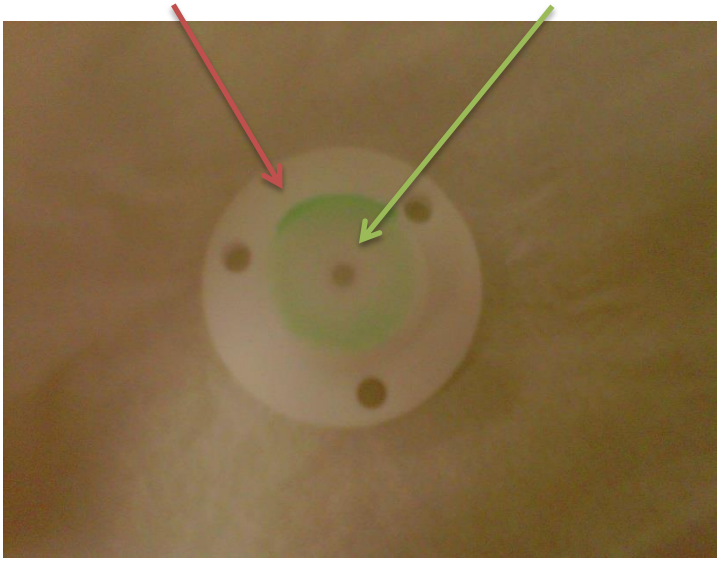

Fig. 6: Photograph of the Teflon and Teflon holder where, red arrow) Teflon holder, green arrow) Teflon sheet with the hole 100 micron attached to the holder with green PDMS. The diameter of the Teflon holder is approximately 25 cm.

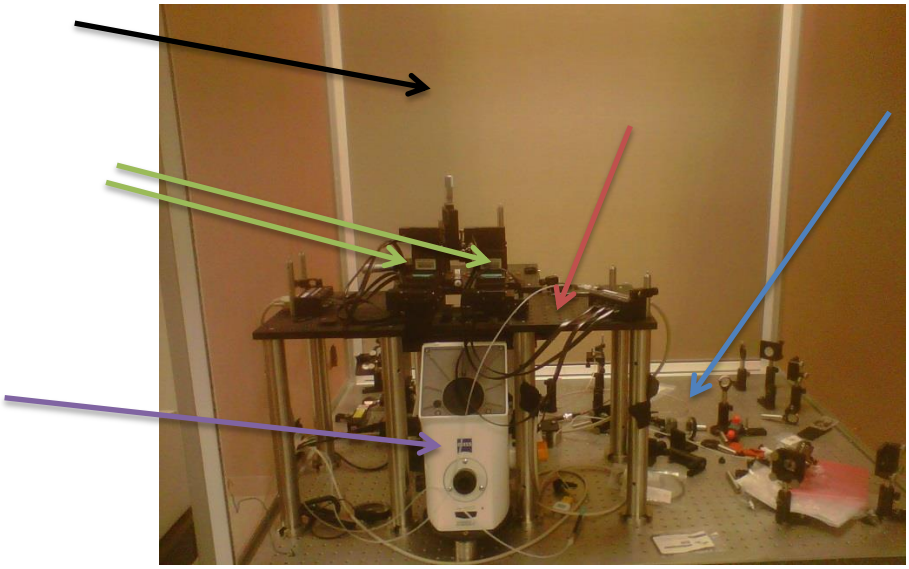

Fig. 7: Photograph of the experimental apparatus where the, black arrow is the faraday cage, green arrow are the manipulators, red arrow is the head stage where the manipulators are attached, blue arrow is the air table to cancel out the noise, and purple arrow is the inverted microscope to view the hole and membrane formation.

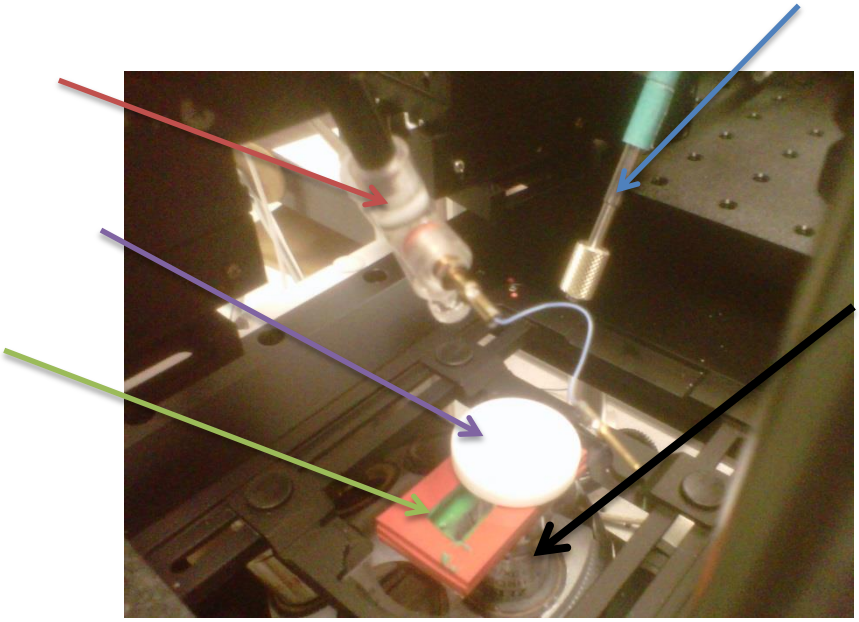

Fig. 8: Zoomed in view of the experimental apparatus where black arrow is the objective of the microscope, purple arrow is the Teflon holder with the Teflon attached, green arrow is the reservoir of the salt and PEG concentration, red arrow is the electrode holder, and blue arrow is a micro injector for the protein and the lipid ejection.

Data Analysis

The lab view code was written in house and uses a threshold discrimination algorithm to identify blockade events where the current is less than 80% of the average open current for at least 100 micro seconds. We than calculate the open state 200 microseconds before and after each event and use these two values to calculate the average value of the open state current and we than calculate the mean current of the blockade and then divide one by the other to create a histogram of $\langle i \rangle / \langle i_o \rangle$ events. We also record the arrival time of every event for the

autocorrelation analysis. Then we perform an autocorrelation on these arrival times by adjusting the binning to optimize the signal to noise ratio of the auto correlation functions.

Chapter 4: Theory

Current Blockades

The most up to date model describing the PEG induced current blockades considers two major contributions. The first contribution is that the current reduction is from the volume exclusion of ions within the pore due to the presence of the PEG. The other contribution is from the binding of cations to the PEG itself. These contributions are described in full detail here {4} from which the following equation was derived to describe the current blockades.

$$\frac{\langle i \rangle}{\langle i_o \rangle} = \left(1 - \frac{L_{PEG}}{L_{pore}}(1-y)\right)^{-1} \qquad (1)$$

where

$$y = \frac{2C_o D_o A_{pore}}{\left(A_{pore} - A_{PEG}\right)\left(C_+ D_+^{eff} + C_- D_-^{eff}\right)} \qquad (2)$$

In equation 1 L_{PEG} defines the average length of the PEG molecule bound to the pore wall, L_{pore} is the total length of the pore, and y is defined by equation 2. In the second equation D_0 and C_0 describe the diffusion coefficient concentrations of the cations and anions respectively and are considered constant in the PEG free region. A_{pore} is defined as the cross sectional area of the pore and A_{PEG} is the average cross sectional area of the PEG molecule. Finally $D^{eff}_{\pm}$ is the effective diffusion coefficient for anions and cations and $C_{\pm}$ is the concentration of the cations and anions in the PEG occupied region of the pore. How these equations are derived is beyond the scope of this thesis, but the take home message is that current blockades occur because of a decrease in the ionic current from a reduction of the concentration of mobile ions inside the pore. This is

caused by both volume exclusion due to the displacement caused by the PEG molecule and by cation complexation with the PEG; this in turn decreases the local diffusion coefficients of the ions in the pore. The effect of this on the magnitude of the current blockades is that they depend on both the size of the PEG molecule and on the applied voltage. The larger the PEG the larger the values of L_{PEG} and the A_{PEG} which would increase the value of $\frac{<i>}{<i_0>}$ and increasing the applied voltage applies a stronger force on the PEG bound cations and will increase the number of events but decrease the residence time of the pore.

Residence Time

In the 2010 PNAS it was proposed that the binding of cations to the PEG molecule led to an increased residence time of the PEG in the pore. This lead to the following Arrhenius-type residence time dependence

$$\langle \tau_n \rangle = \tau_o \exp\left(-\beta\left(n\Delta G_c + m_b\left(\Delta G_o + s^{PEG} e\left|V_{app}\right|\right)\right)\right) \qquad (3)$$

Where τ_0 is the nonbinding diffusion limited residence time of the molecule in the pore. Also m_b is the average number of bound cations to the PEG molecule. Where $n\Delta G_c$ is the confinement free energy of the PEG in the pore and $m_b \Delta G_0$ is the change in free energy of the cations dissociating from the PEG. Finally the term $s^{PEG} e\left|V_{app}\right|$ corresponds to the screened electric force on the PEG molecule from the applied voltage.

From Eq. 3 the free energy dissociation of PEG from the nanopore determines the average residence time of the molecule inside the pore. The original work from the 2010 PNAS hypothesized that the PEG molecules bind to the nanopore by cation association to the polymer, which in turn led to an enhanced binding. However more recent molecular dynamic simulations

suggests a slightly modified interpretation where the PEG does not directly bind to the walls of the pore, but rather, the cation binding to the PEG leads to a lowering of the entropic barrier for the PEG to enter the pore {Ref A Balijepalli et al. accepted for publication in JACS 2013}. This simply refines the residence time interpretation; the important experimental factors that affect the residence time are still the size of the PEG, the concentration of the KCL and the applied voltage. All three of these parameters are explored and found to be consistent with the predictions of the model in Eq. 3, which states as we increase the applied voltage the electric force, is increased and so the residence time is decreased due to the bigger negative exponent in the exponential. Then if we increase the size of the molecule more cations can attach to it which causes an enhanced binding of the molecule to the pore, and increasing the salt concentration will also cause this interaction as well.

Autocorrelation and Translocation

One of the difficulties of nanopore sensing is that you can't see what happens right before and right after an event. Many events in biology use nanopore translocation that transports molecules across membranes. It is difficult to see if a molecule traverses the pore let alone how to measure said events. One indirect method we explore here uses the autocorrelation of PEG arrival times to study the probability of a molecule entering the pore, leaving on the same side that it entered, and reentering the pore. Figure 9 illustrates the concept behind reentry. It relies on the fact that for a voltage driven process, we should see an asymmetry in the probability of the molecules hitting the pore from one side versus the other.

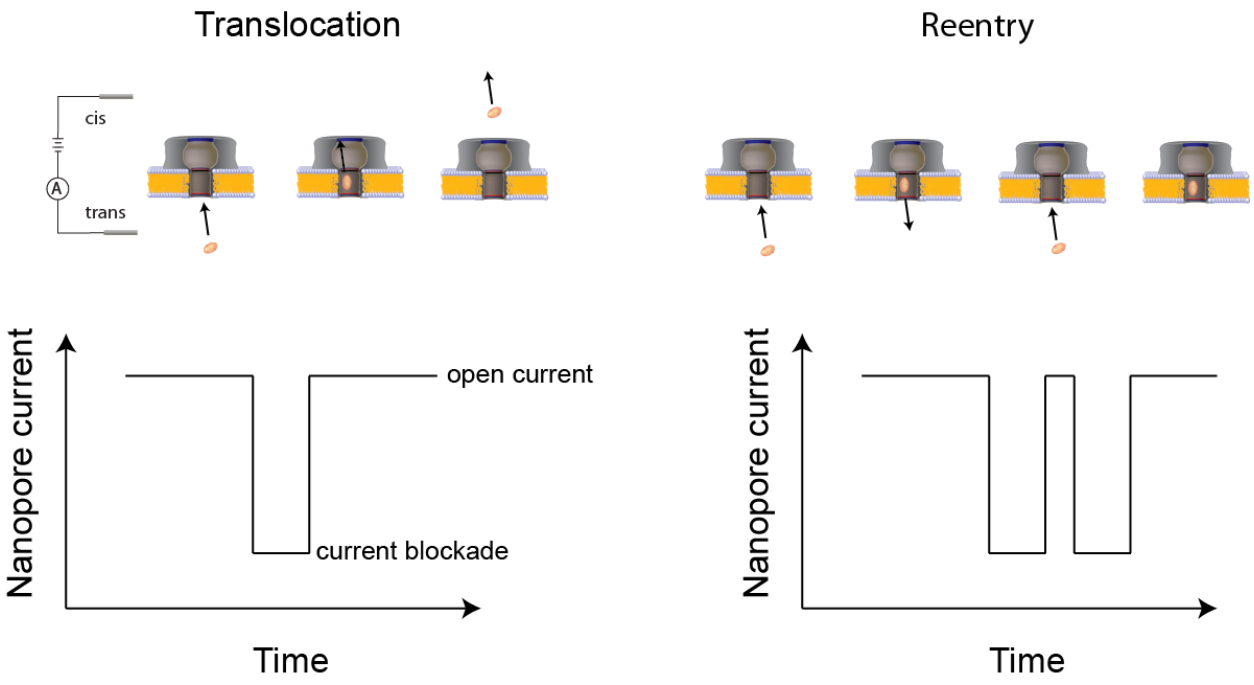

Figure 9: Drawing of a, Left) translocation and Right) reentry, processes as well as the corresponding current blockades. Notice that the blockades for the reentry case are really close to one another. This is because a molecule that transits through the pore should give rise to a single current blockade, but a molecule that exits on the same side it entered has a high probability of reentry that leads to the second blockade.

One way to quantify the likelihood of these reentry events is to measure the probability of an event given a previous event, regardless of what the actual event will be, this is called an autocorrelation and is calculated by creating a histogram of the times between hit events. We recast the entire current stream into the following functional form

$$i(t) \rightarrow I(t) = i_o \sum_k \delta(t - t_k) \qquad (4)$$

Where *i(t)* is the actual current trace, and the right arrow represents a transformation to *I(t)* which is described only by the arrival times t_k of all the PEG molecules. Figure 10 provides an illustration of this process.

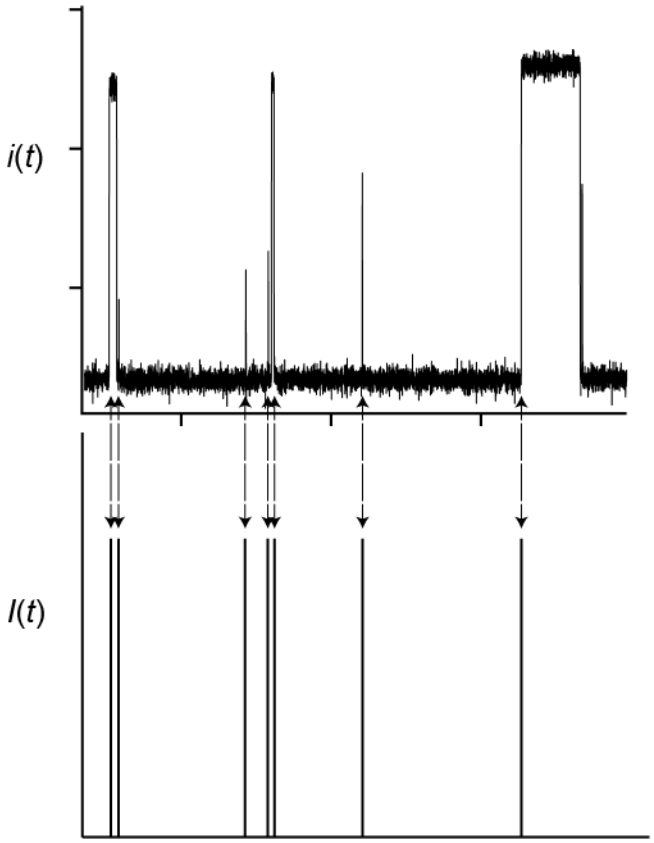

Fig. 10: Top real current trace reproduced from Fig. 4 transformed into a series of delta functions where the value is i_0 only at the arrival time of the PEG molecules, not the exit. From the lower function we can construct the autocorrelation of the arrival times.

The unnormalized autocorrelation function for I(t) is given by.

$$G(t_1,t_2)=\langle I(t_1)I(t_2)\rangle \quad (5)$$

Where the brackets imply a time average. For the PEG data taken throughout this thesis, the current traces are stationary processes. This means the data looks similar no matter where you start from so there is no true t = 0 value to the data. In this case, all that matters is the time difference between an event at t_1 and t_2. Therefore we can recast the autocorrelation function in normalized form as

$$g\left(\tau = t_2 - t_1\right) = \frac{\left\langle I(0) I(\tau) \right\rangle}{\left\langle I \right\rangle^2} \qquad (6)$$

We can use Eq. 6 to calculate the autocorrelation of the PEG nanopore process. First we build an array of the arrival times of all PEG molecules, and then we copy this array into a new array and shift the elements by one. We then subtract this shifted array from the original array. This gives an array whose values are the difference in time between adjacent PEG arrivals. We repeat this process by shifting by another element and subtract this doubly shifted array from the original array. This leads to an array whose values are the difference in time between each event and the secondary event (one after the next event). We repeat this process until the smallest time difference between any two events is greater than the upper limit in tau that we wish to measure. Finally we build a histogram of all these differences which is equivalent to Eq. 6. This was computed using a program that was built in Labview.

From Eq. 6 we can elicit a few details about the processes. At long time differences, the system should have no memory and we should see g = 1. This is consistent with two uncorrelated random events. At short times, the system may have some memory and this is the region of interest. If g > 1, this implies we are detecting more events separated at these short times than we would expect from a truly random process. Evidence of this at short times suggests reentry of the PEG molecules into the pore. If g < 1 than this implies that we are seeing fewer events at this time then we would expect from a random process. Figure 11 provides an illustration of these different regimes.

For a random process it should be one if the events are finite in time and there should be antibunching, so the events should be fairly spaced out. It should be below one at first and then

increase to one. If there is a pronounced peak then there are more events than expected which would suggest reentry which could be used to measure the likelihood of translocation.

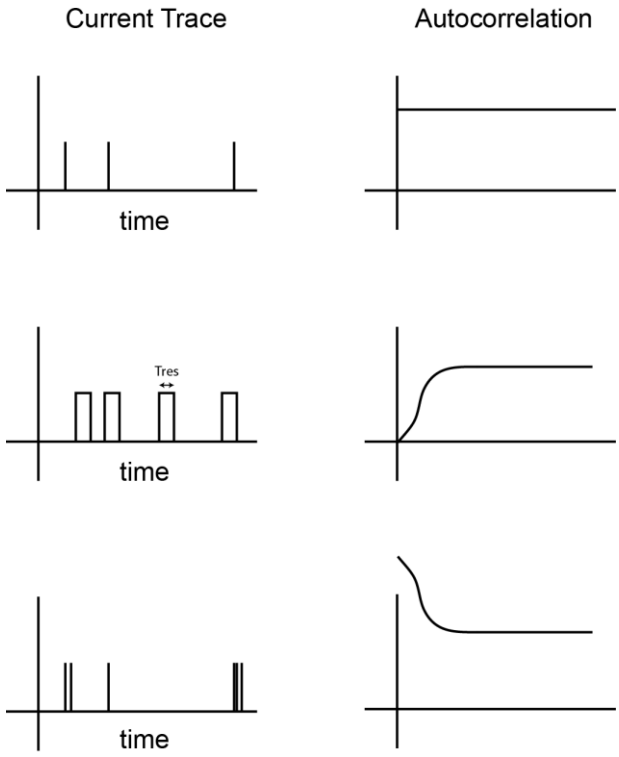

Fig. 11: Top left shows a completely random process where the corresponding autocorrelation on the top right shows G = 1. Middle left shows a series of current blockades with a finite residence time Tres, which leads to a decrease in the number of expected events at short time intervals. The bottom left shows a series of closely bunched events that may arise from molecules exiting and entering the pore in quick succession. This would lead to an increase in the number of events separated by short times and a corresponding peak in the G function at short times.

Chapter 5: Results

Current Blockade Distributions

We mix PEG-29, which is a monodisperse mixture were all the PEG molecules have *n* = 29 repeat monomer units with PEG polydisperse which is a mixture of different size molecules and is named after the average molecular weight of the included molecules, for example PEG 600, 1000, 1500 correspond to PEG mixtures with an average molecular weight of 600, 1000 and 1500 Da respectively. Now the mixtures are combined with PEG-29 so the total concentration of PEG-29 is higher than the concentrations of the other sized PEGs so we should see a higher peak corresponding to PEG-29 then the others which lets us calibrate the current blockade distribution so we know which peak corresponds to which size molecule.

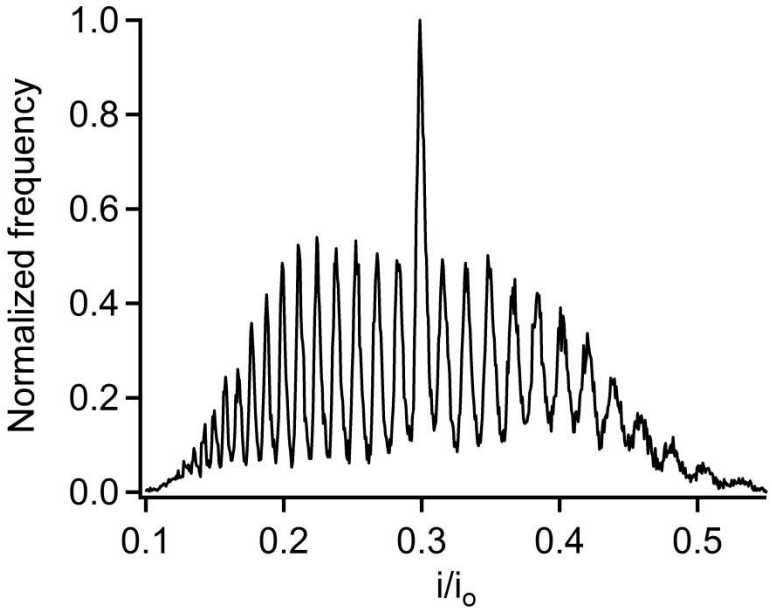

Fig 12: Here is a comb at 3.5M KCL at -40mV applied voltage. PEG 1000, 1500 at 10 µmol/L and PEG 29 at 1µmol/ L.

Here the comb calibrated with the PEG29 which shows us the ability of the pore to resolve individual peaks. We can see that the peak for PEG29 is larger due to the increased concentration of PEG29 compared to other sized PEG molecules. The deeper blockades correspond to larger molecules were each peak corresponds to a differently sized molecule.

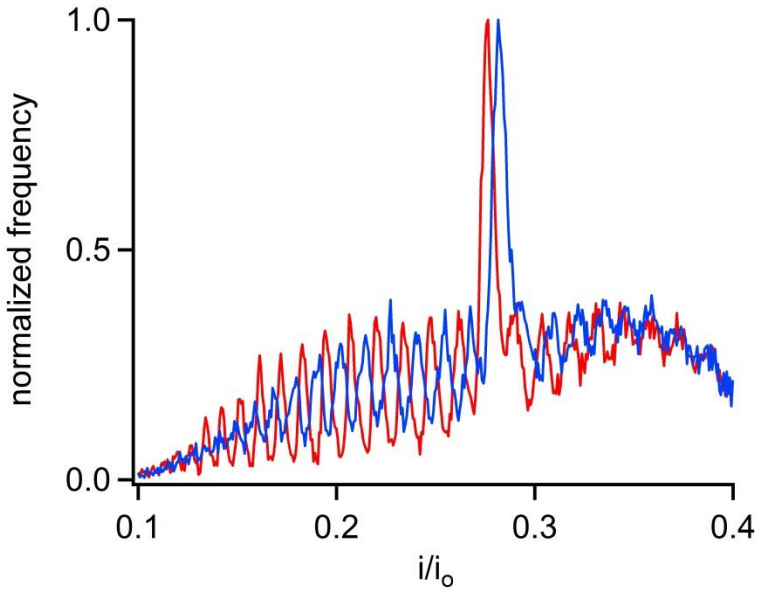

Fig 13: Here is another comb at 3.8M KCL where the red line is at -40mV and the Blue line is at -60mV. PEG 1000 and 1500 at 10µM. PEG 29 = µM we notice that the peak is a bit higher relative to comb here. This implies an ideal PEG 29 concentration is around 0.5 to 1 µM or so. This plot has a limited "visibility" in other peaks.

Here we see two combs overlaid at different voltages. The most important feature is that we can see a shift to the right due to the increasing voltage applied. This shift can be attributed to the cation/PEG binding model {4} were the increased voltage decreases the binding of the cations to the PEG and leads to a decreased reduction in the current. This manifests itself in a rightward shift of the current blockade distribution.

Now at 3M KCL the residence time of the molecule in the pore gets really short so it is difficult to construct a good looking comb so we only show the PEG-29 peaks at 3M KCL which is shown below.

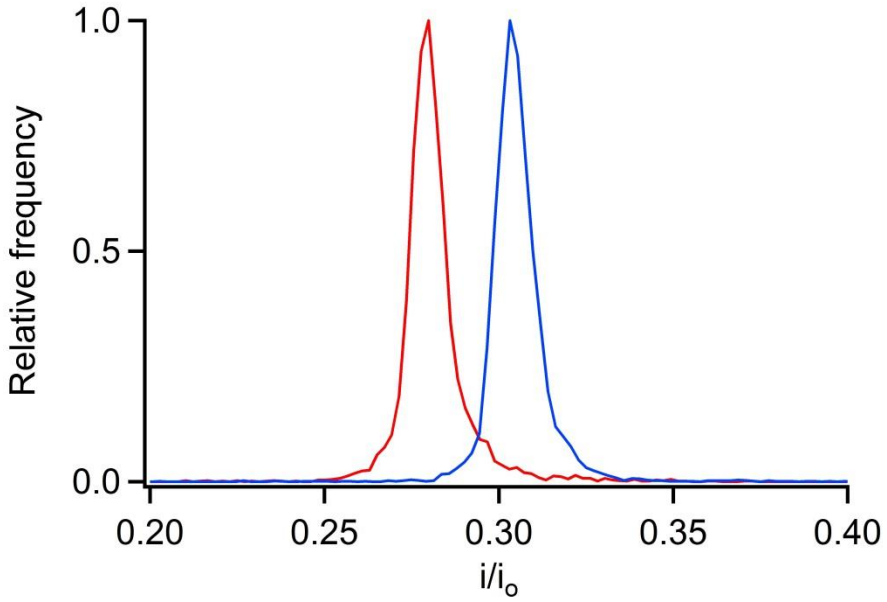

Fig 14: Here's a comb at 3M KCL with N=29 only where the red line is at -40mV and the blue line is at -80mV. 20 µM of PEG 29. We notice a clear shift in the peak position with applied voltage which is consistent with model describing cation binding in the pore {4}

The shift of the combs caused by the voltage can be more clearly seen at the 3M concentration with only the N-29 peaks present. We can clearly see that there is shift to the right at a higher applied voltage of -80mV compared to the smaller voltage of -40mV.

Residence Time Distributions

Residence time distributions for the PEG molecules in the nanopore are found calculating all residence times of each event within a particular peak in the blockade distributions. We assign an *n* value from the *n* = 29 calibration and create a histogram of the results.

Figure 10 shows two residence time distributions for small (n=20) and large (n=40) PEG molecules on log-log scale with fit functions.

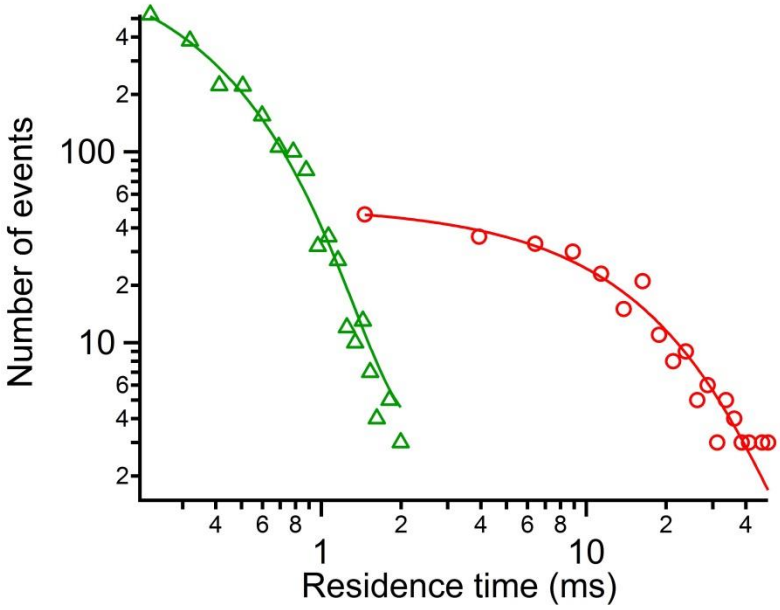

Fig. 15: Distributions of lifetimes at two different sized PEG molecules. KCL concentration = 3.8M Green N = 20, tau = 0.30 ms. Red N =40 tau = 13 ms. Fit with a function $y = y_0 + A*\exp(-(t-t_0)/tau)$. Solid lines are fits, open symbols are data.

So now if we look at the voltage dependence of residence time we see that as voltage decreases the residence time increases.

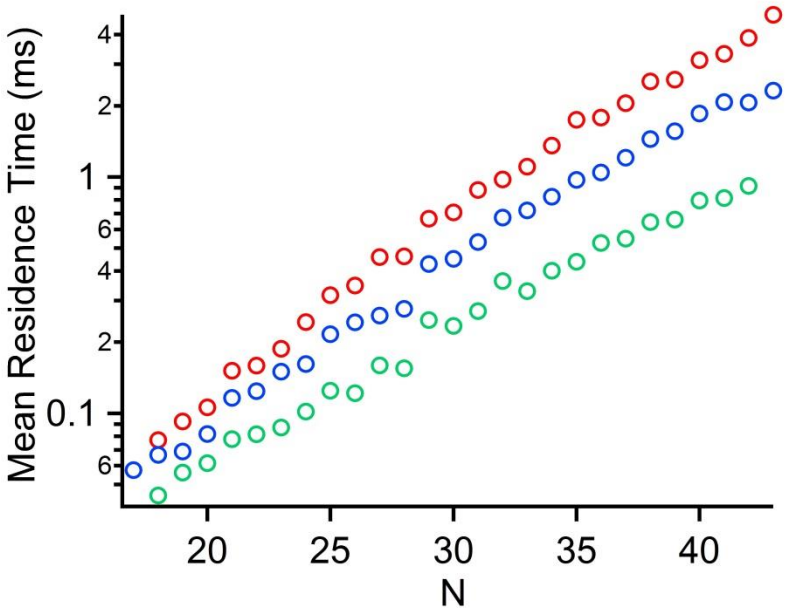

Fig 16: Here is the residence time versus different sized molecules at 3.5M KCL and a different applied voltage where red is -40mV, blue is -60mV, and green is -80mV. Same data as figure 7, but this shows the -60 and -80 mV data too.

The above graph shows the effects that voltage dependence has on the residence time. The voltage dependence is most likely due to increase rate of dissociation of the cations from the PEG molecule at higher voltages. This means that the PEG molecule detaches itself from the pore faster which lowers the residence time of the molecule in the pore.

From the above graph we also see that the residence time also depends upon the size of the PEG molecule. As the size of the molecule increases there is increased surface area for the cations to bind to so there is a higher charge placed on these molecules which means that it takes longer for the cations to sufficiently decrease enough for the PEG to be released from the pore. This is counter intuitive from an entropy argument where you would expect that larger molecules would want to escape the confined space of the pore.

Now we look at the residence time at different salt concentrations and different PEG size were bigger PEG molecules are longer. The two most important adjustable parameters that affect the residence time of the PEG in the pore are the salt concentration and the applied voltage.

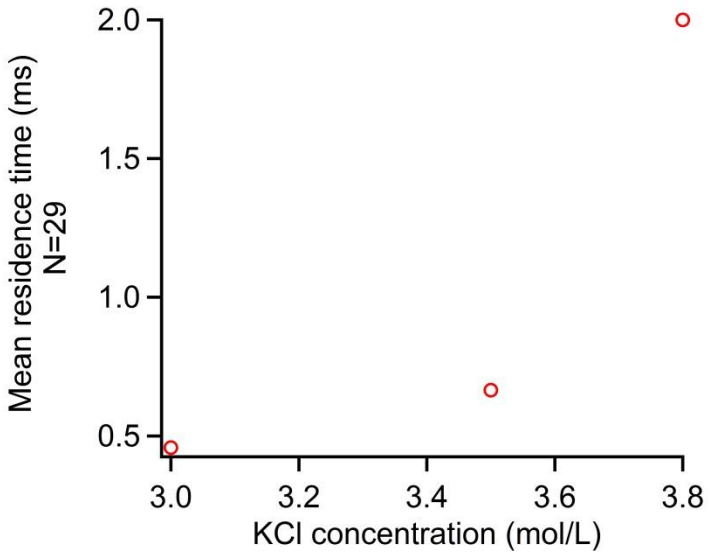

Fig 17: Residence time of the molecule in the pore versus the concentration of KCL for N=29 only.

This figure shows that the residence time increases exponentially with the increasing salt concentration for n = 29. This implies that there is cation binding to the PEG molecules and with increasing cation concentration we see more cations binding to the PEG and then when the PEG enters the pore it spends an increasing amount of time within the pore. When enough of the bound cations dissociate from the PEG it is released from being attached to the pore and the PEG exits the pore so a higher concentration of PEG results in a higher localized concentration on the PEG which means that the PEG is attached to the pore for a longer period of time.

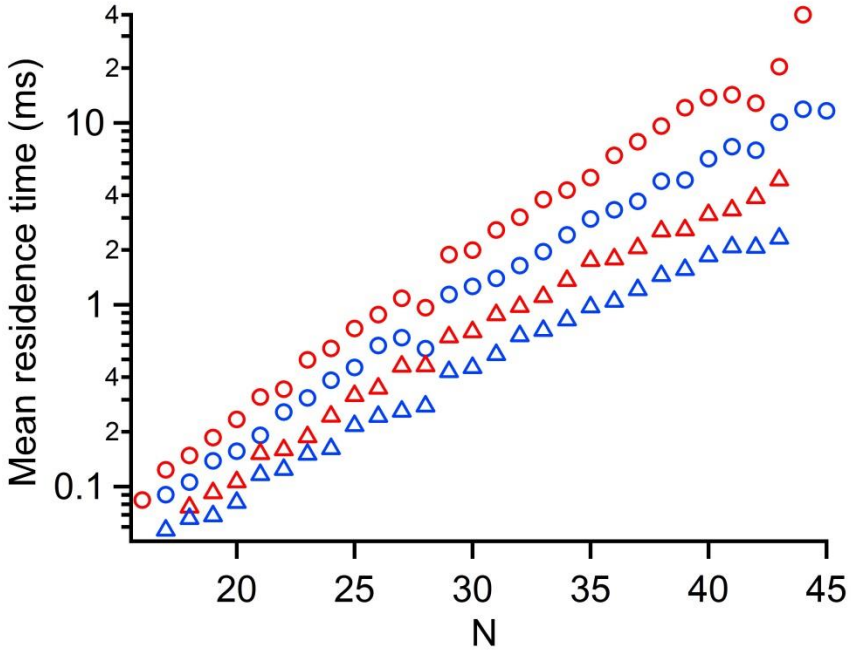

Fig 18: Here is the residence time versus different sized molecules at 3.8M KCL (circles), and 3.5M KCL (triangles) and a different applied voltage where red is -40mV, blue is -60mV.

This graph combines the two previous graphs by showing us the residence time dependence on salt concentration, applied voltage, and size dependence of the molecule.

PEG Arrival Autocorrelation

At lower concentrations the likelihood of subsequent events is decreased due to a smaller localized concentration of target molecules. The arrival times of the PEG molecules should follow a Poisson distribution, but if molecules are exiting and reentering the pore from the same side then we should see more arrivals than expected at short intervals. This can be observed by calculating the autocorrelation of the arrival times and seeing if it is a truly random process.

Here we define the autocorrelation of the arrival time as $G(\tau) = \langle I(t_1)\, I(t_2)\rangle = \langle I(0)\, I(t_2 - t_1 = \tau)\rangle$ where we assume a stationary process were $t_1 = 0$ is irrelevant because the system looks similar at all times. I(t) represents a delta function which equals one for an arriving photon and

zero at all other times. For a truly random process G = G (0) and will have no time dependence, and for a process that has more events than was expected G > G (∞) and for fewer events G < G(∞).

The curve below shows the autocorrelation for concentration of 20 µM of PEG 29 at -80mV and at -100mV. We see antibunching at first which is in agreement with the residence time behavior, namely, the events have a finite duration, which precludes the existence of repeats at short times less than the residence time. In fact, the measured residence times are consistent with the decay times seen in these figures. More importantly, there is no overshoot suggesting the number of event-s is too large for us to detect the superpoissonian re-entry behavior.

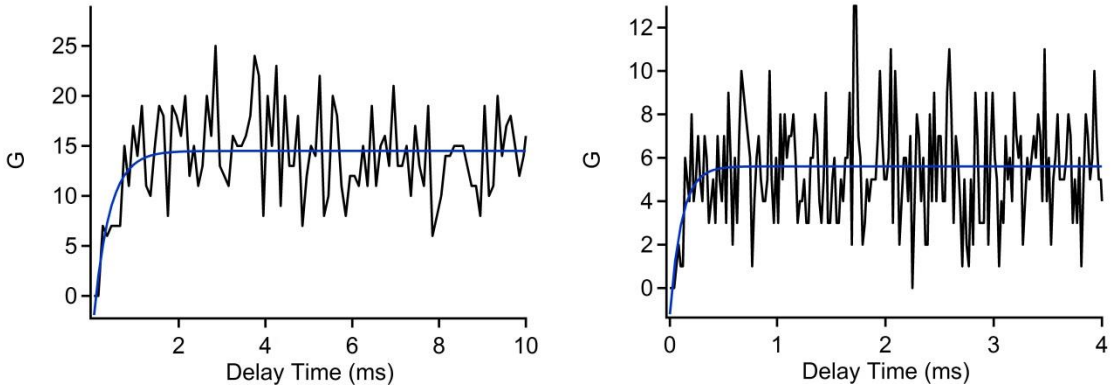

Fig 19: Autocorrelation of the PEG arrival times at a high concentration of PEG. Left) is at -80mV applied voltage from which we see a rise time of (367 ± 130) microseconds. Right) is at -100mV applied voltage with a rise time of (108 ± 42) microseconds. PEG 29 concentration is 20 µM for both plots, 3 M KCL.

The lack of a peak near zero implies that there is no evidence of bunching, so we cannot see reentries over the top of the arrival of other PEG molecules.

Here is a plot with a lower concentration and we can see that there is no initial overshoot. The concentration of PEG is only 1 µM so the number of events is much lower than the previous

case. However due to the decrease in events the statistics are not as clear as before, but the evidence of a peak near the zero delay time suggests a bunching of events which may suggest the reentry of molecules.

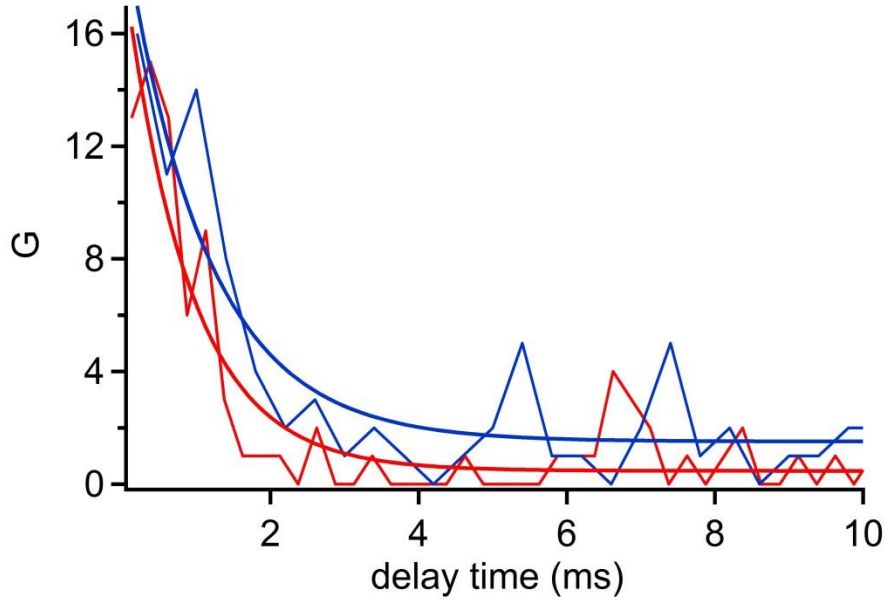

Fig 20: The PEG 29 concentration is at 1 micro molar. The applied voltages are -80mV (red) and -100mV (Blue). The fall times are 0.9 ± 0.1 microseconds for the -100mV data. 3 M KCL

The presence of peaks at t=0 for the lower concentration is due to more events occurring immediately following another molecule. This can possibly be the pore bound molecule drifting out of the pore and right back into the pore within a very short time frame.

We now consider the following calculation for a PEG concentration of 1μM, which mean that the molecule can be considered to be confined to a 100 nm^3 "box". Assuming the PEG leaves, than the time to diffuse outside of this "box" can be given roughly by the following.

$dT = dx^2/6D$ where dT is time, dx is 100nm, and D is the diffusion coefficient which for PEG 29 we can assume to be $2.5e^{-10}$ m^2/s. We can now calculate the value for dT which is roughly 6.67

μs. This is a bit faster than what we observe in the bunching shown in Fig. 20, but we don't know exactly why the hit rate is so much lower than was predicted by Berg and Purcell {13}. They said that the hit rate should be given by 2DCr, where D equals the diffusion coefficient, C is the concentration and r is the radius of the nanopore. From this we find that the rate should be about 1000 hits/s at 1 μM concentration when in fact we observe approximately 1 hit/s. It's possible that the local concentration of PEG at the pore is not as high as we think; perhaps the membrane is slightly charged which leads to a reduction in the PEG concentration. Nevertheless, if we use the concentration of 1 nM as predicted from the hit rate of PEG molecules to the pore then from the diffusion equation above we find that dT is closer to 900 μs which is more consistent with what we see in the exponential decay in figure 20. More work is required to address these issues.

Chapter 6: Conclusion

From the performed measurements, we verified that the data received from PEG interactions with the pore we are able to create a mass spectrometry comb of PEG and have shown its voltage dependence. We can also see the dependence that the salt concentration has on the residence time of the PEG molecule in the pore. We also explored a new type of analysis with the autocorrelation measurement of the nanopore. Also if there is reentry occurring then it must be happening faster than 20 micro seconds which is faster than we can see.

This work has also set up the lab to have single molecule nanopore capabilities. Future work will involve coupling this analysis to verify thermodynamics of other processes besides PEG molecules, such as DNA unzipping and other low transition temperature polymers.

Works Cited

1. Zlatanova, Jordanka, and Kensal Van Holde. "Single-Molecule Biology: What Is It and How Does It Work?" *Molecular Cell* 4 (2006): 317-29. Web.
2. Henrickson, Sarah E., Martin Misakian, Baldwin Robertson, and John J. Kasianowicz. "Driven DNA Transport into an Asymmetric Nanometer-Scale Pore." *Physical Review Letters* 85.14 (2000): 3057-060.
3. Kasianowicz, John J., Eric Brandin, Daniel Branton, and David W. Deamer. "Characterization of Individual Polynucleotide Molecules Using a." *Natl. Acad. Sci.* 93 (1996): 13770-3773. Web.
4. Reiner, J. E., J. J. Kasianowicz, B. J. Nablo, and J. W. F. Robertson. "Theory for Polymer Analysis Using Nanopore-based Single-molecule Mass Spectrometry." *Proceedings of the National Academy of Sciences* 107.27 (2010): 12080-2085. Web.
5. Kumar, Shiv, Chuanjuan Tao, Minchen Chien, Brittney Hellner, Arvind Balijepalli, Joseph W.F. Robertson, Zengmin Li, James J. Russo, Joseph E. Reiner, John J. Kasianowicz, and Jingyue Ju. "PEG-Labeled Nucleotides and Nanopore Detection for Single Molecule DNA Sequencing by Synthesis." *Scientific Reports* 2 (2012): Web.
6. Song, Langzhou, Michael R. Hobaugh, Christopher Shustak, Stephen Cheley, Hagan Bayley, and J. Eric Gouaux. "Structure of Staphylococcal α-Hemolysin, a Heptameric Transmembrane Pore." *Science* 274.5294 (1996): 1859-866. Web.
7. Dekker, Cees. "Solid-state Nanopores." *Nature Nanotechnology* 2.4 (2007): 209-15. Web
8. "Ethylene Glycol - PubChem." *Ethylene Glycol - PubChem*. N.p., n.d. Web. 10 Apr. 2013.
9. Lee, Hwankyu, Richard M. Venable, Alexander D. MacKerell Jr., and Richard W. Pastor. "Molecular Dynamics Studies of Polyethylene Oxide and Polyethylene Glycol: Hydrodynamic Radius and Shape Anisotropy☆." *Biophysical Journal* 95.4 (2008): 1590-599. Web.
10. "Polyethylene Glycol." *Wikipedia*. Wikimedia Foundation, 13 Apr. 2013. Web. 14 Apr. 2013.

11. Robertson, J. W. F., C. G. Rodrigues, V. M. Stanford, K. A. Rubinson, O. V. Krasilnikov, and J. J. Kasianowicz. "Single-molecule Mass Spectrometry in Solution Using a Solitary Nanopore." *Proceedings of the National Academy of Sciences* 104.20 (2007): 8207-211.
12. CE Angevine, N. Kothalawala, A. Dass, JE Reiner, "Characterizing individual $Au_{25}(SG)_{18}$ clusters within a nanopore detector," *MRS Proceedings*. 1484. (2012). Doi:10.1557/opl.2012.1625
13. Berg, H., and E. Purcell. "Physics of Chemoreception." *Biophysical Journal* 20.2 (1977): 193-219. Web.